

Isodeformation curves of the extraocular muscles from the inverse kinematics of a cable-driven parallel kinematics mechanism model of the eye

Carlos Andrés Trujillo Suárez

Profesor, Departamento de Ingeniería Mecánica, Universidad de Antioquia, Medellín, Colombia

Correo-e: carlos.trujillo@udea.edu.co

Abstract—A mechanical model of the eye considering it as a cable-driven parallel kinematics mechanism is proposed. The inverse kinematics of the eye is carried out and the isodeformation curves of the extraocular muscles are obtained. The results agree with those previously reported by other, more complex, analytical approaches and with physiological measurements. This effort is a contribution to the modeling of the kinematics of the eye from the standpoint of robotics and mechanism theory and it could be used in eye movement studies to explore brain function. This work may support the neurologically-constrained argument for the positioning of the eye.

Keywords—Extraocular muscles, inverse kinematics, isodeformation curves.

I. INTRODUCTION

The human eye is a sophisticated biological device whose motion obeys well established physiological rules such as Listing's law (LL) [1, 2, 3] and Sherrington's law of reciprocal innervation [4]. LL, for instance, describes the change of orientation of the eye as if the pupil traveled along a great arc starting at a reference position. It is an issue of lively controversy among physiologists whether this is a neural or mechanical phenomenon [5, 6, 7].

Analytical approaches to model the kinematics of the eye have been proposed; however, some of these works focus on describing the geometry involved without referring to the extraocular muscles (EOM) [8, 9], while others are aimed to the design of robotic eyes, using simplifications which do not describe the actual behavior of the EOMs, or they are not intended to predict the interplay between the EOMs [10, 11].

Theoretical approaches to describe the behavior of the EOMs are reported in the literature. Boeder proposed a model that predicts the contractive states of the muscles using analytic geometry considerations [12]. A classical paper by Robinson computes the force required in each muscle to keep the eyeball in static equilibrium at a prescribed gaze direction; an empirical relationship is used to numerically calculate the

length and innervation of each EOM [13]; a computer application that allows to plot iso-innervation curves, among other plots, has been developed based on this theory [14]. Wei et al. simulated the EOMs as strands, i.e. splines with inertia, based on which equations of motion are obtained and, through an optimization procedure, the EOM innervations are computed [15]. More recently, finite element models (FEM) of the extraocular muscles have been proposed to describe the mechanical properties of the eye under static force tests and the medial rectus force for a specific orientation of the eye [16]. However, the FEM and the optimization-based approaches are not meant to model how motion planning of the eye is performed by the brain and rely on initial guesses of muscle innervation. It is not clear whether the brain performs such a task.

From the standpoint of robotics and mechanism theory, the kinematics of the eye and the interplay between the EOMs is a motion planning problem, which can be modeled based on techniques commonly used in these fields, such as the theory of parallel robots [17]. This paper proposes a mechanical model of the eye considering it as a cable-driven parallel kinematics mechanism, for which, the inverse kinematics is carried out. From this procedure, the deformation state of the EOMs required for any gaze direction is obtained and isodeformation plots are constructed. The results agree with those previously reported by other, more complex, analytical approaches, as previously discussed, and with physiological measurements. They may also support the claim that motion planning of the eye is neurologically rather than mechanically determined. The effort developed here may prove as a simpler, yet useful contribution to the modeling of the kinematics of the eye and to the understanding of the motion planning by the brain. This methodology could be used to develop plausible models in eye movement studies, which have gained renewed interest as a convenient alternative to evaluate brain function, since there is a need of modeling frameworks in this area given the limitations of physiologically invasive experiments [18].

II. ANATOMY AND PHYSIOLOGICAL LAWS OF EYE ROTATION

In this section, a description of the anatomy of the EOMs and the physiological rules that are observed in normal eye movements are presented, as far as to what pertains to this paper.

A. Extraocular muscles.

The human eye is driven by three pairs of agonist and antagonist extraocular muscles, which allow for the orientation of the eyeball in the desired gaze direction. The superior rectus (SR) and the inferior rectus (IR) have the main function of pointing the eyeball upwards, i.e. supraduction, and downwards, i.e. infraduction, respectively; the lateral rectus (LR) and the medial rectus (MR) move the eye outwards, i.e. abduction, and inwards, i.e. adduction, respectively; the superior oblique (SO) and the inferior oblique (IO) rotate the eye torsionally, the SO executes internal torsion towards the nose, i.e. intorsion, and the IO extorsion, as described in figure 1 for a right eye.

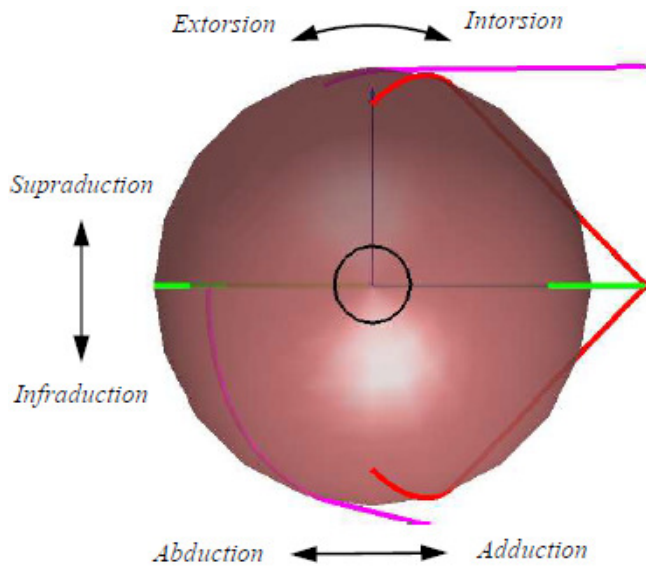


Figure 1. Movements of the right eyeball as seen from the front of the face.

Most orientations of the eyeball require the action of more than one EOM; therefore, the interplay between these muscles allows for the positioning of the eyeball, which is about 24 mm in diameter. Table 1 lists the actions in which each EOM is involved. The first action is the one where the corresponding muscle is the main actuator and the others are the secondary actions of the muscle.

All recti originate at the Annulus of Zinn and are about 40 mm long at their resting length. The SO originates above the Annulus of Zinn and passes through the trochlea, a structure that acts as a pulley fixed to the socket of the eye on the

frontal bone; the IO originates at the lacrimal fossa. The insertion points of the SR and IR are slightly beyond the north and south poles of the eyeball, correspondingly. The insertion of the LR and MR is also past the poles along the equator of the eyeball. The SO inserts into the eyeball behind the north pole; the IO farther behind the south pole. There are anatomic measurements of the coordinates of the origin and insertion points reported elsewhere in the literature [19].

Muscle	Action
Superior rectus	Supraduction
	Adduction
	Intorsion
Inferior rectus	Infraduction
	Adduction
	Extorsion
Lateral rectus	Abduction
Medial rectus	Adduction
	Intorsion
Superior oblique	Infraduction
	Abduction
	Extorsion
Inferior oblique	Supraduction
	Abduction

Table 1. Action of extraocular muscles.

Figure 2 depicts the extraocular muscles of a right eye as wire segments. Each EOM wraps the globe on a great arc, L_s , between its insertion and tangency points and reaches its origin through the straight-line segment L_r . In this figure, only the segment of the SO that goes from the trochlea to the insertion in the eyeball is shown since the length of the segment from the trochlea to the origin of this muscle remains fixed.

B. Listing’s law and Sherrington’s law.

LL states that any gaze direction the eye is pointing to, is such as if it was achieved by a rotation starting from a reference position, called the primary position, following a great arc on the sphere of the eyeball. This law implies that all the vectors about which these rotations occur lie on a single plane, called Listing’s plane. Referring to figure 3, \mathbf{z} is the direction of the primary position, usually assumed when the eye is looking straight ahead; \mathbf{s} is the unit vector representing the gaze direction at a secondary position; \mathbf{n} is the unit rotation vector, perpendicular to \mathbf{z} and \mathbf{s} , which lies on Listing’s plane; the pupil moves along a great arc, centered at the center point C of the eyeball, an angle θ .

Since, geometrically, there are multiple paths that could be followed by the eye in order to end at a given gaze direction and, thus, with different torsion, i.e. the orientation about the direction of sight, but the brain chooses the one specified by LL, there is active controversy whether this is a phenomenon determined by neurological or mechanical factors [5, 6, 7].

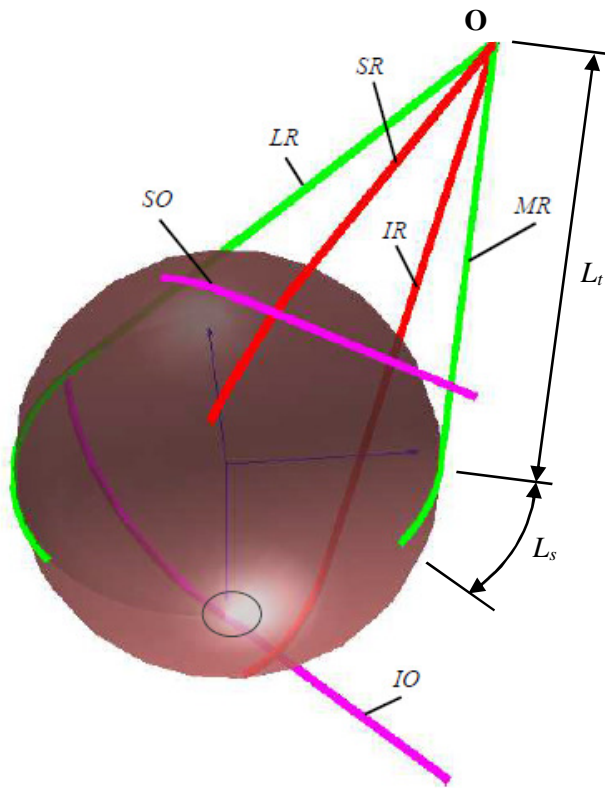


Figure 2. The extraocular muscles of the right eye. Each EOM wraps the globe on a great arc, L_s , between corresponding insertion and tangency points, and reaches its origin through the straight-line segment L_t .

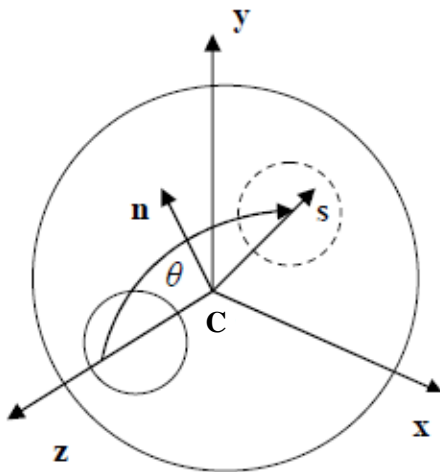


Figure 3. Listing's law.

There is another well-known physiological fact called Sherrington's law of reciprocal innervation. This law entails that while one EOM is innervated, the agonist, its antagonist is relaxed. Sherrington's law is demonstrated by means of electromyography (EMG), and not only is it observed in the

EOMs but also in other agonist-antagonist pairs of muscles in the body [4].

III. INVERSE KINEMATICS OF THE EYE

This section briefly describes the representation of rotations by means of quaternions. Then, the inverse kinematics of the eye is carried out using quaternions to represent the orientation of the eye according to Listing's law.

A. Quaternions.

A unit quaternion $\mathbf{q} = q_1i + q_2j + q_3k + q_4$, representing the rotation of a rigid body by an angle θ about the unit axis vector $\mathbf{n} = (n_1, n_2, n_3)$, is built upon the so-called Euler-Rodriguez parameters of the rotation

$$q_1 = n_1 \sin \frac{\theta}{2}, q_2 = n_2 \sin \frac{\theta}{2}, q_3 = n_3 \sin \frac{\theta}{2}, q_4 = \cos \frac{\theta}{2}. \quad (1)$$

These components satisfy the relation $q_1^2 + q_2^2 + q_3^2 + q_4^2 = 1$. The quaternion basis units obey the fundamental multiplication rules $i^2 = j^2 = k^2 = ijk = -1$.

The Cartesian coordinates of a point $\mathbf{x} = (x_1i, x_2j, x_3k, 0)$, written as a quaternion, are transformed to the coordinates $\mathbf{X} = (X_1i, X_2j, X_3k, 0)$ after the rotation represented by the unit quaternion \mathbf{q} , by the quaternion product $\mathbf{X} = \mathbf{q}\mathbf{x}\mathbf{q}^*$, where $\mathbf{q}^* = -q_1i - q_2j - q_3k + q_4$ is the conjugate of \mathbf{q} .

Quaternions are geometrically intuitive rotation operators and suitable for computational implementation; thus, in this work, they are preferred to other representations. A deeper treatment of quaternions can be found in theoretical kinematics textbooks [20, 21].

B. Procedure and algorithm.

According to LL and referring to figure 3, the orientation of the eye from the primary position, pointing in the direction of the unit vector \mathbf{z} , to a position where the eye is looking at, pointing in the direction of the unit vector \mathbf{s} , is achieved by a rotation an angle θ about the unit axis vector \mathbf{n} perpendicular to both, the primary position \mathbf{z} and the gaze direction \mathbf{s} . This rotation can be described by a quaternion \mathbf{q} as previously discussed. Considering the eyeball a rigid body, all of its points must perform the same rotation represented by \mathbf{q} , including the insertion point of each EOM on the globe.

Therefore, applying this rotation, using the quaternion product, to the coordinates of the insertion points of the EOMs in the primary position, will result in their coordinates after the rotation. Then, the length of each of the EOMs in the final position, or gaze direction, can be computed as the sum of the arc length of the great arc on the eyeball, connecting the insertion and tangency points of a given muscle, and the length from the tangency point to the origin of the muscle, \mathbf{O} ;

L_s and L_t , respectively, in figure 2. This procedure will render the length of each EOM required to achieve a desired orientation.

The procedure just described assumes that the EOMs accommodate on the globe along a great arc; however, magnetic resonance imaging (MRI) studies have shown that the actual path of the muscles is affected by restraining tissue, called active pulleys, that slightly changes the location of the insertion and tangency points dependent on gaze direction, causing that the muscle does not wrap the sphere along a great arc [22].

It must be noted that the eye is a mechanical system with three degrees of freedom, which are required to position the pupil in a desired orientation. This can be shown by employing the mobility equation for compliant mechanisms [23, 24, 25]. However, an equivalent pseudo-rigid-body model allows to use the Grubler-Kutzbach criterion for mechanisms with rigid links [26]:

$$M = 6(n - 1) - \sum_{i=1}^5 (6 - i)f_i \quad (1)$$

where M is the mobility or number of degrees of freedom, n is the number of links and f_i is the number of joints with i degrees of freedom.

Using the latter approach, considering the wires representing the EOMs as equivalent prismatic (P) joints and their insertion and origin points as spherical (S) joints, the eye has six P joints, thirteen S joints, including the coupling of the globe on the eye socket, and fourteen links: the eyeball, the orbit, and the links joined by the P joints of the EOMs. Plugging these values into the Grubler-Kutzbach equation a mobility of nine is obtained. However, six degrees of freedom are passive, i.e. the twist of the cables around their own axis, resulting in the three degrees of freedom as was already foretold.

Therefore, only the three EOMs with the maximum shortening are the ones that should be innervated in order to achieve the desired orientation.

The algorithm has been implemented in MATLAB® for a right eye of radius $r = 12$ mm and the center of the globe as the origin of coordinates, as illustrated in figure 3, in terms of the horizontal gaze angle θ_h , positive for adduction, negative for abduction, and the vertical gaze angle θ_v , positive for supraduction, negative for infraduction, both relative to the primary position. The procedure can be summarized as follows:

- Compute gaze direction vector, $\mathbf{s} = (\cos \theta_v \sin \theta_h, \sin \theta_v, \cos \theta_v \cos \theta_h)$.
- Compute unit axis vector and angle of the rotation, $\mathbf{n} = (\mathbf{z} \times \mathbf{s}) / \|\mathbf{z} \times \mathbf{s}\|$, $\theta = \cos^{-1}(\mathbf{z} \cdot \mathbf{s} / (\|\mathbf{z}\| \|\mathbf{s}\|))$.

- Assemble unit quaternion \mathbf{q} .
- Compute location of insertion points \mathbf{i} of each EOM after the rotation according to quaternion product.
- Compute angle θ_i between vector from center of the globe to tangency point and vector from the center, \mathbf{C} , to the origin, \mathbf{O} , of the EOM, $\theta_i = \cos^{-1}(r / \|\mathbf{O}\|)$.
- Compute angle θ_t between vector from center of the globe to insertion point and vector from the center to the origin of the EOM, $\theta_t = \cos^{-1}(\mathbf{i} \cdot \mathbf{O} / (\|\mathbf{i}\| \|\mathbf{O}\|))$.
- Compute arc length of EOM segment wrapped around the globe, $L_s = r(\theta_i - \theta_t)$; refer to figure 2.
- Compute length of EOM segment from tangency point to origin of the muscle, $L_t = \sqrt{\|\mathbf{O}\|^2 - r^2}$.
- Compute deformation of EOM, $\Delta L = (L_s + L_t) - L_o$, where L_o is the EOM length at primary position.

The coordinates of the insertion points at reference position used in this paper, for each of the EOM, are presented in table 2. These coordinates are relative to a coordinate system centered at the right eyeball as depicted in figure 3. The Annulus of Zinn, which is the common origin for all recti, has coordinates $\mathbf{O}_{ZIN} = (15; 0; -32)$ in mm. The trochlea, which is the origin of the SO neglecting the segment that remains constant from the trochlea to the Annulus of Zinn, has the coordinates $\mathbf{O}_{SO} = (15; 12; 8)$ and the origin of the IO, at the lacrimal fossa, has the coordinates $\mathbf{O}_{IO} = (11; -15; 11)$.

Muscle	Coordinates in mm
Superior rectus	(0; 10; 6.65)
Inferior rectus	(0; -10; 6.65)
Lateral rectus	(-10; 0; 6.65)
Medial rectus	(9.65; 0; 7.14)
Superior oblique	(-2.65; 11; -4)
Inferior oblique	(-9; 0; -7.94)

Table 2. Insertion points at reference position of EOM.

IV. RESULTS AND DISCUSSION

The previous calculation was carried out on each of the EOMs for a span of gaze angles, horizontal as well as vertical, between -20° and 20° and isodeformation curves were plotted using the *contour* command in MATLAB®. Each isodeformation line is in mm. See figure 4.

These curves reflect the actions of the EOMs as described in table 1. Clearly, the main role of the recti muscles is on the region of the corresponding graph where the muscles have

negative deformation, i.e., contraction. They also show that the superior and inferior recti have a share on adduction whether the eye is looking up or downwards, respectively. It is also shown that the superior and inferior obliques are contracted during infraduction and supraduction, respectively, which are their secondary actions. Moreover, the three innervated muscles required to achieve a given gaze direction can be determined from the curves. For instance, when the eye is looking upwards and away from the nose, i.e., supraduction and abduction, the three actuators are the SR, the LR and the IO; when the eye is looking downwards and towards the nose, i.e., infraduction and adduction, the three actuators are the IR, the MR and the SO. There are gaze directions where up to four muscles are contracted, e.g., when looking all the way towards the nose, i.e., total adduction, the MR, the SR, the IR, and the IO would be contracted; however, only three degrees of freedom are required; this is what is known in robotics as a redundancy. Even though this paper does not attempt to speculate how the brain deals with redundancy, from a practical point of view, the three largest deformations would be enough to position the eye in the desired orientation.

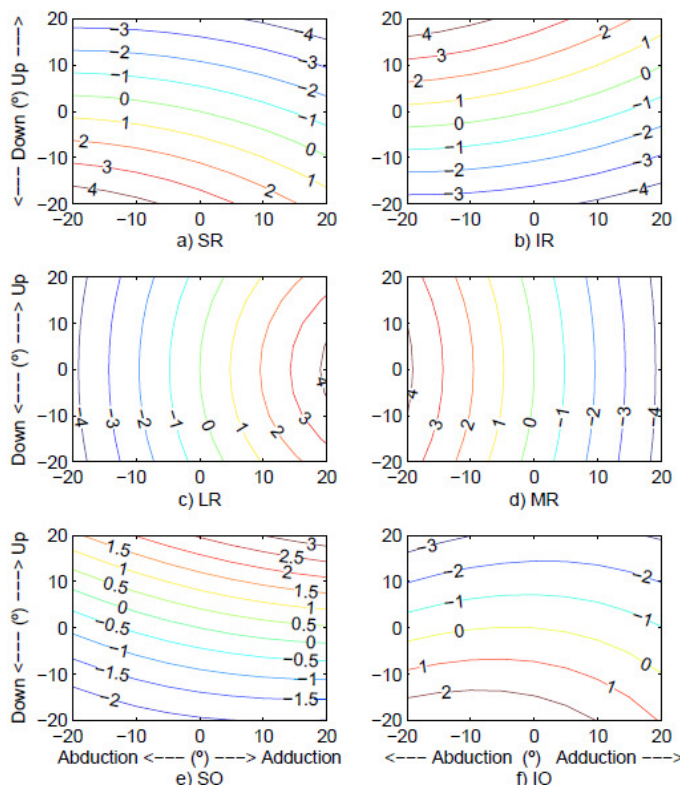


Figure 4. Isodeformation curves of EOMs of a right eye; level curves in mm.

It must be noticed that the pattern observed in the isodeformation curves is similar to that of isoinnervation curves obtained from electromyography (EMG) measurements in monkeys [27], as well as to the patterns obtained by more complex approaches, as discussed in

Section I. For instance, figure 5 shows the results for the forces of the recti by the method proposed by Robinson [13], which considers the positioning of the eye at a desired orientation as a static equilibrium problem; it entails to solve a linear system of nine equations and nine unknowns, i.e. the magnitude of each of the six extraocular muscle forces and the three components of the moment exerted by passive tissue that returns the eye to the primary position, for each orientation. There is arguably an advantage of the methodology developed in the present paper since no system of linear equations is required to solve.

Furthermore, the level of deformations is in the range of values reported by MRI studies in healthy subjects [28].

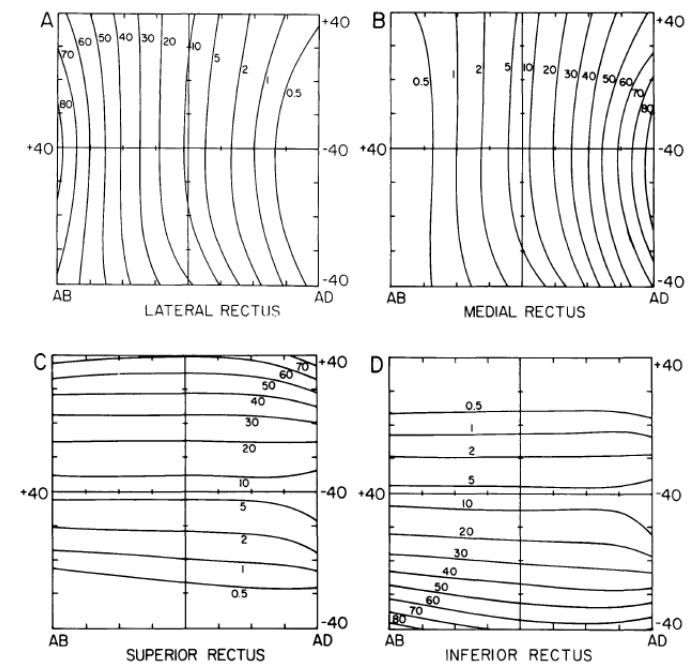


Figure 5. Equi-innervation (force) curves of EOMs of a right eye; level curves in g. [13]

In general, Sherrington's law is also evident in the plots. Whenever the SR is contracted, the IR is not, and vice versa; this reciprocity is also observed between the LR and the MR. There are regions where Sherrington's law seems to be violated; but again, mechanical redundancy of the eye can explain those exceptions. This interplay is also observed between the SO and the IO; however, their main action being torsion is not visualized in these plots.

The procedure previously exposed incorporates Listing's law a priori, just to make it in accord with the physiological facts observed in normal eyes. However, from a motion planning perspective, different criteria could be implemented in order to achieve a desired orientation. Therefore, this may suggest that LL is neurologically rather than mechanically dictated.

V. CONCLUSIONS

This paper presents an approach for the kinematic modeling of the eye considering it as a cable-driven parallel kinematics mechanism. The inverse kinematics for such a mechanism was developed and isodeformation curves of the extraocular muscles were obtained. Assumptions were made that deviate from the actual eye, such as: the consideration of the eyeball as a rigid body, the wrapping of the EOMs along a great arc on the globe and neglecting active pulleys. Nevertheless, the patterns and the results agree with those reported in the literature by other, more complex, analytical approaches and with EMG measurements. Moreover, the methodology here described is in accord with the physiological laws observed in the normal eye.

To the best of our knowledge, this is the first time that the theory of parallel kinematics mechanisms has been applied to obtain isodeformation curves of EOMs. This is a contribution to the kinematics modeling of the eye and to the understanding of the motion planning by the brain from the standpoint of robotics and mechanism theory. The approach described here may be used in eye movement studies, which have gained renewed interest as a convenient alternative to evaluate brain function. As a matter of fact, there is a need of modeling frameworks for eye movement research given the limitations of invasive experiments, thus, the methodology proposed here could be useful for that purpose. Finally, this work may support the neurologically-constrained argument for the implementation of Listing's law and the positioning of the eye.

ACKNOWLEDGMENTS

The support of the Alternative Energy Group (GEA) of University of Antioquia is highly appreciated.

REFERENCES

- [1]. Tweed D, Vilis T. "Geometric relations of eye position and velocity vectors during saccades". *Vision Research*, 30(1), pp. 111–127, 1990.
- [2]. Bolina O, Monteiro L. "Kinematics of eye movement". *Ophthalmic and Physiological Optics*, 20(1), pp. 59–62, 2000.
- [3]. Skalicky SE. "Movements of the eye". In: *Ocular and Visual Physiology*. Springer; 2016, pp. 243–249.
- [4]. Wright KW. "Anatomy and physiology of eye movements". In: *Pediatric Ophthalmology and Strabismus*. Springer; 2003, pp. 125–143.
- [5]. Angelaki DE. "Three-dimensional ocular kinematics during eccentric rotations: evidence for functional rather than mechanical constraints". *Journal of Neurophysiology*, 89(5), pp. 2685–2696, 2003.
- [6]. Crawford J, Martinez-Trujillo J, Klier E. "Neural control of three-dimensional eye and head movements". *Current Opinion in Neurobiology*, 13(6), pp. 655–662, 2003.
- [7]. Demer JL. "Current concepts of mechanical and neural factors in ocular motility". *Current Opinion in Neurology*, 19(1), pp. 4–13, 2006.
- [8]. Haslwanter T. "Mathematics of three-dimensional eye rotations". *Vision Research*, 35(12), pp. 1727–1739, 1995.
- [9]. Bayro-Corrochano E. "Modeling the 3D kinematics of the eye in the geometric algebra framework". *Pattern Recognition*, 36(12), pp. 2993–3012, 2003.
- [10]. Cannata G, Maggiali M. "Models for the design of bioinspired robot eyes". *IEEE Transactions on Robotics*, 24(1), pp. 27–44, 2008.
- [11]. Wang XY, Zhang Y, Fu XJ, Xiang GS. "Design and kinematic analysis of a novel humanoid robot eye using pneumatic artificial muscles". *Journal of Bionic Engineering*, 5(3), pp. 264–270, 2008.
- [12]. Boeder P. "Co-operative action of extraocular muscles". *The British Journal of Ophthalmology*, 46(7), pp. 397–403, 1962.
- [13]. Robinson DA. "A quantitative analysis of extraocular muscle cooperation and squint". *Investigative Ophthalmology & Visual Science*, 14(11), pp. 801–825, 1975.
- [14]. Miller J, Pavlovski D, Shaemeva I. *Orbit 1.8 Gaze Mechanics Simulation - User's Manual*. San Francisco: Eidactics, 1999. URL: <http://www.eidactics.com/projects/ooi/>; (retrieved Jan. 18, 2019).
- [15]. Wei Q, Sueda S, Pai DK. "Physically-based modeling and simulation of extraocular muscles". *Progress in Biophysics and Molecular Biology*, 103(2), pp. 273–283, 2010.
- [16]. Karami A, Eghtesad M. "Simulation of active eye motion using finite element modelling". *Latin American Journal of Solids and Structures*, 15(3), e24. Epub May 14, 2018.
- [17]. Merlet JP. *Parallel Robots*. 2nd ed., The Netherlands: Springer, 2006.
- [18]. Shaikh A, Zee D. "Eye movement research in the twenty-first century—a window to the brain, mind, and more". *The Cerebellum*, 17(3), pp. 252–258, 2018.
- [19]. Krewson 3rd WE. "The action of the extraocular muscles: a method of vector analysis with computations". *Transactions of the American Ophthalmological Society*, 48, pp. 443–486, 1950.
- [20]. Bottema O, Roth B. *Theoretical Kinematics*, New York: North-Holland Publ. Co, 1979.
- [21]. McCarthy JM. *Introduction to Theoretical Kinematics*. MIT press, 1990.
- [22]. Kono R, Clark RA, Demer JL. "Active pulleys: magnetic resonance imaging of rectus muscle paths in tertiary gazes". *Investigative Ophthalmology & Visual Science*, 43(7), pp. 2179–2188, 2002.
- [23]. Ananthasuresh G. "How far are compliant mechanisms from rigid body mechanisms and stiff structures?" In: *Advances in Mechanisms, Robotics and*

Design Education and Research, Springer; 2013, pp. 83–94.

- [24]. Howell LL, Ananthasuresh G. “Cases studies and a note on the degrees of freedom in compliant mechanisms”. In: *Proceedings of the 1996 ASME Design Engineering Technical Conferences and Computers in Engineering Conference*, pp. 18–22, August, 1996.
- [25]. Murphy M, Midha A, Howell LL. “On the mobility of compliant mechanisms”. In: *Proceedings of the 1994 ASME Design Technical Conferences*, pp. 475–479.
- [26]. Howell LL, Midha A. “A method for the design of compliant mechanisms with small-length flexural pivots”. *ASME Journal of Mechanical Design*, 116(1), pp. 280–290, 1994.
- [27]. Hepp K, Henn V. “Isofrequency curves of oculomotor neurons in the rhesus monkey”. *Vision Research*, 25(4), pp. 493–499, 1985.
- [28]. Piccirelli M, Luechinger R, Rutz AK, Boesiger P, Bergamin O. “Extraocular muscle deformation assessed by motion-encoded MRI during eye movement in healthy subjects”. *Journal of Vision*, 7(14), pp. 1–10, 2007.